

Design and experimental testing of a gas cluster ion accelerator^{*}

Xiao-Mei Zeng(曾晓梅) Vasily Pelenovich Chuan-Sheng Liu(刘传胜) De-Jun Fu(付德君)¹⁾

Key Laboratory of Artificial Micro- and Nano-Materials of Ministry of Education and Hubei Nuclear Solid Physics Key Laboratory, School of Physics and Technology, Wuhan University, Wuhan 430072, China

Abstract: A gas cluster ion beam (GCIB) system with cluster energy up to 12 keV has been designed. To facilitate pumping of the nozzle chamber and increased pressure of the gas source up to 10 atm, pulse mode was used for the gas feeding. Argon was employed as the working gas. To separate monomers from clusters, both electromagnet and retarding electrode were utilized. A maximal pulsed cluster current of 90 nA has been achieved. The shape of pulsed ion beam currents has been analyzed in detail at different applied magnetic and retarding electric fields.

Keywords: gas cluster ion beam, flow visualization, cluster mass separation, retarding electrode

PACS: 36.40.Wa, 41.75.Ak, 41.85.Qg **DOI:** 10.1088/1674-1137/41/8/087003

1 Introduction

A cluster is a particle of sub-nanometer or nanometer scale, which consists of several to several thousand atoms. When accelerated clusters interact with a solid-state surface, the large number of atoms in the cluster results in some particular features, which are noticeably different from those of atomic or molecular beams. Among these are very high energy density and temperature in the impact zone, high mass-to-charge ratio, lateral sputtering effect, multiple scattering phenomena, and the ability to transport more material using the same beam current [1]. The lateral sputtering effect has been found to be responsible for the surface smoothing of the target by the cluster beam [2], as well as for unusual angular distribution of the sputtered particles [3]. The high mass-to-charge ratio allows reduction of the Coulomb repulsion of the particles in the beam during its transport to a target.

Cluster beams, which can be produced from solid, liquid or gaseous materials, are widely applied to modern physics experiments: shallow p-n junction formation, low damage surface modification and etching [4], ultra-smooth surface formation [5, 6], high sputtering yield processes [3, 7], and high quality inorganic thin film formation [8, 9].

Ion beam techniques and equipment have made great progress during the last few decades, reaching cluster ion beam current of 1 mA [10]. It was found that for practical applications cluster formation using supersonic ex-

pansion is the best way to obtain high intensity cluster beams [11], and the efficiency of the cluster formation strongly depends on the nozzle geometry [12]. The first gas cluster ion beam (GCIB) equipment developed for industrial applications was constructed by the Yamada group in the early 1990s [13]. In 1997, Epion Corporation developed the first commercially available GCIB equipment for surface cleaning and smoothing, ultra-shallow implantation, film formation, sputtering, etc. [14, 15].

The number of atoms in the nozzle-generated clusters depends on the source pressure and is in a wide range from several hundred to several thousand [1]. To obtain the mass distribution of the cluster beam, retarding electric field and time-of-flight (TOF) techniques are mostly used. In the first method, the difference of the kinetic energy of the clusters is used. The kinetic energy can be considered as proportional to the size of the cluster, hence different retarding fields are required to stop clusters of a certain masses [12]. The TOF technique is a direct way to measure the velocity of the clusters, and therefore their mass. If it is only necessary to remove monomers and light clusters, a simple permanent magnet can be used [16].

In this study we describe the design of a gas cluster ion accelerator with a gas source working in pulse mode, which facilitates effective pumping of the vacuum system. Such a pulse mode reveals observation of heavy clusters using an electromagnet or retarding electrode to separate (deflect) monomers.

Received 14 February 2017, Revised 5 April 2017

^{*} Supported by International Cooperation Program of the Ministry of Science and Technology of China (2015DFR00720), Wuhan Municipal Science and Technology Bureau (2016030409020219), Suzhou Scientific Development Project (ZXG201448) and Hubei Province Technological Innovation Project (2016AHB004)

¹⁾ E-mail: djfu@whu.edu.cn, Corresponding author

©2017 Chinese Physical Society and the Institute of High Energy Physics of the Chinese Academy of Sciences and the Institute of Modern Physics of the Chinese Academy of Sciences and IOP Publishing Ltd

2 Experimental setup

In Fig. 1, a schematic diagram of the gas cluster ion accelerator is shown. It consists of three chambers: nozzle, ionizer, and processing chambers, separated by two diaphragms. All three chambers are pumped by a turbomolecular pump: a 2000 L/s pump for the nozzle chamber and 700 L/s pumps for the other chambers. The high-pressure gas pipe is connected with a 0.2 mm nozzle via a pulse valve, which is used for pulsed gas feeding [17]. The valve operates at 1–5 Hz with the on-off ratio 5%–50%. Such a mode facilitates the vacuum conditions in all chambers of the accelerator and allows the use of higher pressure in the gas source. The chamber pressures are 1.5 Pa in the nozzle chamber and 10^{-3} Pa in the processing chamber at full gas supply. As working gases Ar, CO₂, and N₂ are used with the source pressure in the range of 1–10 atm. Here, we discuss only results obtained for Ar gas, as it is the most commonly used for surface cleaning, smoothing, and etching.

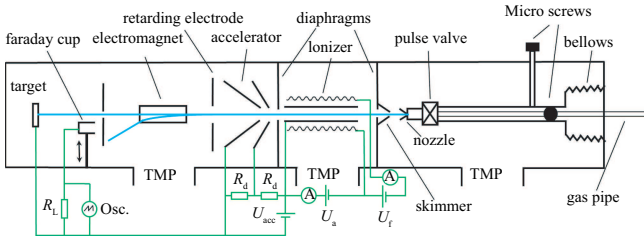


Fig. 1. Schematic and circuit diagram of the gas cluster ion accelerator.

The ionizer is used to ionize the obtained clusters, followed by acceleration and detection. It consists of a cylindrical gauze anode, two tungsten wire cathodes, and a cylindrical shield. The anode of the ionizer is connected with the high-voltage power supply and mounted on the diaphragm through a boron nitride insulating disk. The acceleration voltage U_{acc} applied to anode is in the range of 2–12 kV. The electron emission current generated by the ionizer is 40 mA at the filament current of 1.4 A and anode voltage of 200 V. The accelerator is made of an extractor and a ground electrode. A potential of $-U_{\text{acc}}/20$ relative to the anode is applied to the extractor. The accelerator forms a beam of 2 mm in diameter.

To separate heavy clusters from monomers and light clusters, two techniques have been used: an electromagnet with magnetic field up to 100 mT, and a retarding electrode. In a magnetic field, the Lorentz force affecting the ions is described by the formula:

$$F = q(u \times B), \quad (1)$$

where

$$u = \sqrt{\frac{2qU_{\text{acc}}}{m}} \quad (2)$$

is the velocity of ions with charge q and mass m accelerated by voltage U_{acc} and deflected by a magnetic field with induction B . The heavier the clusters, the smaller the deflecting Lorentz force, so only heavy clusters can be passed to the Faraday cup.

The retarding electrode is mounted after the ground electrode of the accelerator, supplied by positive voltage U_{ret} , which is close to U_{acc} , and provides deceleration of the beam particles.

3 Results and discussion

Cluster formation mostly takes place in the volume near the Mach disk where the temperature of the gas is the lowest, which promotes the condensation process of the gas during the adiabatic process [18]. To position the nozzle relative to the skimmer in the plane perpendicular to the gas flow, two microscrews are used. To find the optimum position we used dependence of the gas pressure on the nozzle transverse displacement relative to the skimmer, as shown in Fig. 2.

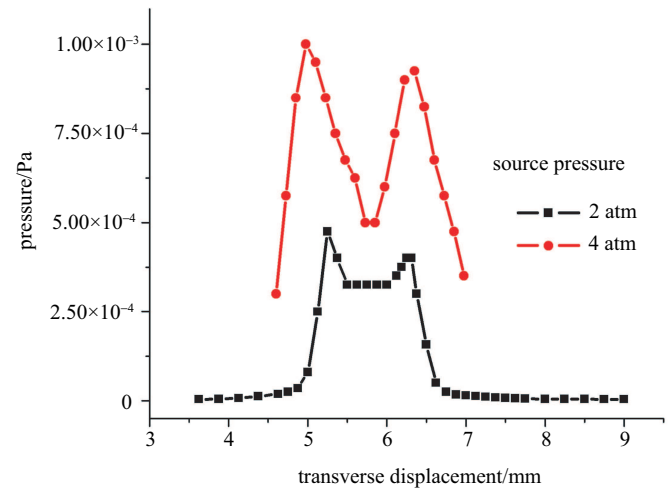


Fig. 2. (color online) Gas pressure in the processing chamber as a function of nozzle position relative to the skimmer.

The two observed maxima are from the intersection of the jet shock waves by the skimmer, so the minimum represents the central axis of the gas jet, where the cluster formation takes place. At higher source pressure, the observed dependence is more prominent.

The optimal longitudinal position of the nozzle relative to the skimmer has been found by a method of visualization of the nozzle jet in glow discharge described in [19, 20]. We removed the ionizer and both diaphragms and applied a voltage of +700 V to the extractor. The jet from the nozzle at a gas pressure in the chamber of 2 Pa and discharge current of 2 mA is shown in Fig. 3.

Similar to previous studies, the Mach disk is observed near the tip of the converging conical shock wave.

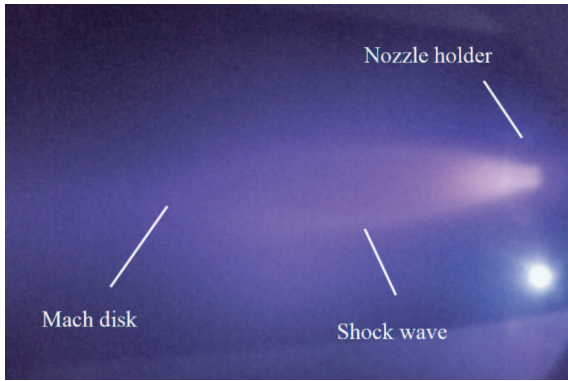


Fig. 3. Jet visualization in glow discharge.

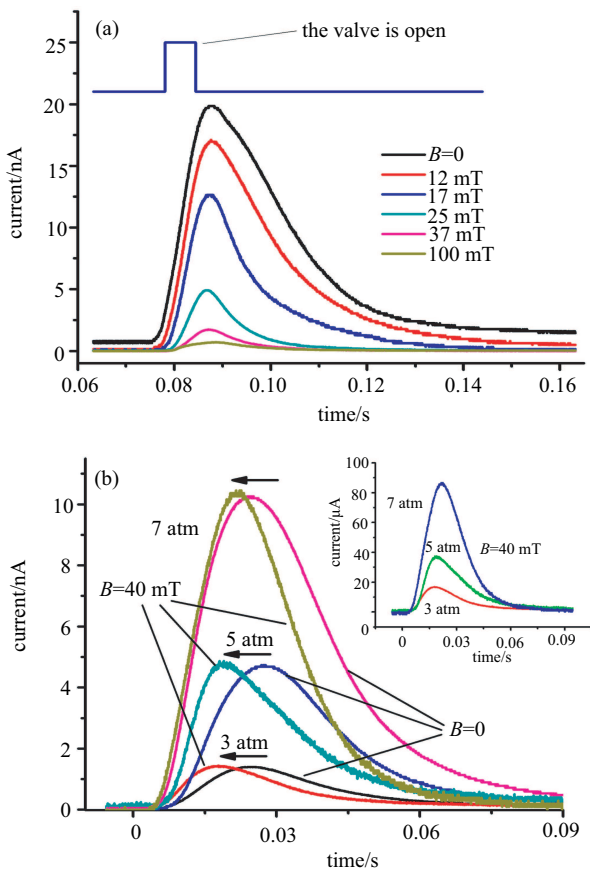


Fig. 4. (color online) (a) Pulses of the ion current passed through various magnetic field strengths and (b) Pulses of the ion current passed through magnetic field at different source pressures normalized to the pulses without magnetic field. Arrows represent the shift of the maxima. The real ion current passed through magnetic field at different source pressures is shown in the inset.

Figure 4(a) shows pulses of the ion current measured by the Faraday cup after passing the electromagnet. Without magnetic field, when the valve is open, the ion current quickly increases up to $20 \mu\text{A}$. Then, when the valve is closed, the current relatively slowly decreases; such a decrease represents a gas release from the finite volume before the nozzle orifice (buffer volume). When the field is applied, a decrease of the pulse amplitude is observed, which proves the deflection of the monomers and light clusters by the Lorentz force. At higher magnetic field B heavier clusters can be deflected by the Lorentz force, see formulas (1, 2), which results in decrease of the cluster ion current detected by the Faraday cup.

In Fig. 4(b), current pulses without and with magnetic field at different source pressures are shown. The intensity of the pulses with magnetic field were normalized to the intensity of the pulses without the field corresponding to the same source pressure, to facilitate their comparison. A maximal cluster current of about 90 nA is observed at the source pressure of 7 atm , see inset. A shift of the maximum of the peaks to the left (earlier moments) takes place when the magnetic field is applied and the shift is larger for lower source pressure. Such a change can prove the presence of the clusters in the beam pulse, since the cluster formation takes place at high source pressure when the valve is open. Moreover, the lengthy right shoulders of each peak with magnetic field suggest that the cluster formation keeps going after the valve is already closed, since the gas pressure in the buffer volume of the nozzle is still high enough to produce clusters. In addition, the shift of the maxima is more evident for lower source pressure; it can also testify to the presence of the cluster formation, since on the one hand lighter clusters are formed at lower pressures, but on the other hand decrease of the pressure in the buffer volume of the nozzle takes place earlier at lower pressure.

Similar behavior is observed when the retarding field technique is used, as shown in Fig. 5. In this case, an appropriate retarding electric field decelerates the monomers and repels them back, but decelerated clusters still can pass through the field. It should be noted that the kinetic energy of the monomers and clusters includes both thermal and accelerating contributions. The latter is equal for monomers and clusters, since the particles pass through the same potential. The thermal contribution for clusters depends, however, to first approximation, linearly on the number of monomers and exceeds the thermal kinetic energy of monomers by a few tens of eV for clusters with 1000 atoms ($\sim 40 \text{ meV}$ per monomer at room temperature). 1000 atoms per cluster is a typical number at which the distinctive features of the cluster – surface interaction appear. In our experiment, we

estimate cluster sizes of more than 100 atoms per cluster using known trajectories of the clusters of each mass and the geometry of the magnetic field and the Faraday cup with the diaphragm.

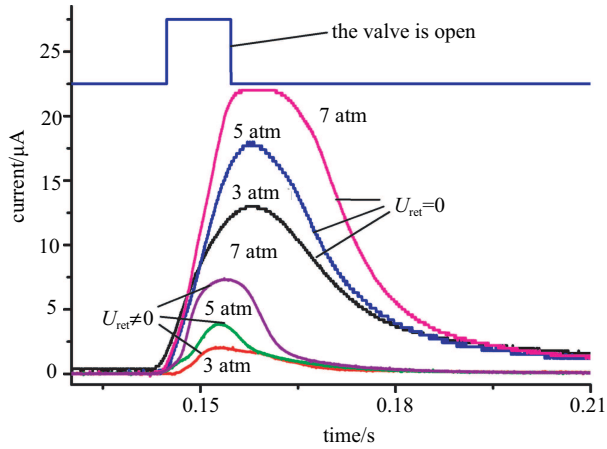


Fig. 5. (color online) Pulses of the ion current passed through electrodes ($U_{\text{ret}} \neq 0$) and pulses without retarding at different source pressure.

4 Conclusion

A gas cluster ion accelerator with cluster ion energy up to 12 keV has been constructed. As working gases, Ar, N₂, and CO₂ are employed. However, the experimental results in this work were presented for Ar gas only since it is the most commonly used for surface cleaning, smoothing, and etching procedures. A gas supply in pulse mode has been designed. Such a mode allows increasing the source pressure up to 10 atm as well as improving vacuum conditions in comparison with continuous mode. Visualization of the nozzle jet in glow discharge and dependence of the pressure in the processing chamber on the transverse displacement of the nozzle relative to the skimmer are used to optimize the nozzle position. Gas pulses formed by a pulse valve are measured by a Faraday cup. The pulsed cluster current is about 90 nA. Distinctive changes of the pulse shape have been observed when separation of the monomers from clusters by electromagnet or retarding electrode takes place; such changes are interpreted as evidence of cluster formation.

References

- I. Yamada, J. Matsuo, N. Toyoda et al, *Mater Sci. Eng. R*, **34**: 231 (2001)
- T. Yamaguchi, J. Matsuo, M. Akizuki et al, *Nucl. Instr. Meth. B*, **99**: 237 (1995)
- N. Toyoda, H. Kitani, N. Hagiwara et al, *Mater. Chem. Phys.*, **54**: 262 (1998)
- A. Kirkpatrick, *Nucl. Instr. Meth. B*, **206**: 830 (2003)
- H. Chen, F. Chen, X. M. Wang et al, *Appl. Phys. Lett.*, **87**: 103504 (2005)
- J.-H. Song, D.-K. Choi, W.-K. Choi, *Nucl. Instr. Meth. B*, **196**: 275 (2002)
- K. Ichiki, S. Ninomiya, Y. Nakata et al, *Appl. Surf. Sci.*, **255**: 1148 (2008)
- T. Kitagawa, I. Yamada, N. Toyoda et al, *Nucl. Instr. Meth. B*, **201**: 405 (2003)
- N. Toyoda, I. Yamada, *Surf. Coat. Tech.*, **201**: 8620 (2007)
- T. Seki, J. Matsuo, *Nucl. Instr. Meth. B*, **237**: 455 (2005)
- E. W. Becker, K. Bier, and W. Henkes, *Z. Physik*, **146**: 333 (1956)
- O. F. Hagen, W. Obert, *Chem. Phys.*, **56**: 1793 (1972)
- J. Matsuo, H. Abe, G. H. Takaoka et al, *Nucl. Instr. Meth. B*, **99**: 244 (1995)
- A. Kirkpatrick and J. Greer, *AIP Conf. Proc.*, **475**: 405 (1999)
- M.E. Mack, *AIP Conf. Proc.*, **576**: 991 (2001)
- N. Toyoda, J. Matsuo, I. Yamada, *Nucl. Instr. Meth. B*, **216**: 379 (2004)
- A. A. Andreev, V. S. Chernysh, Y. A. Ermakov et al, *Vacuum*, **91**: 47 (2013)
- G. Tejada, B. Mate, J. M. Fernandez-Sanchez et al, *Phys. Rev. Lett.*, **76**: 34 (1996)
- N. G. Korobeishchikov, V. V. Kalyada, P. A. Skovorodko et al, *Vacuum*, **119**: 256 (2015)
- A. Ieshkin, Y. Ermakov, V. Chernysh et al, *Nucl. Instr. Meth. A*, **795**: 395 (2015)